Excluded-Volume Effects in Polymer Solutions. 2. Comparison of Experimental Results with Numerical Simulation Data

William W. Graessley*,† and Ryan C. Hayward

Department of Chemical Engineering, Princeton University, Princeton, New Jersey 08544

Gary S. Grest‡

Corporate Research Science Laboratories, Exxon Research & Engineering Company, Annandale, New Jersey 08801, and Sandia National Laboratories, Albuquerque, New Mexico 87185-1411

Received December 11, 1998; Revised Manuscript Received March 15, 1999

ABSTRACT: The effect of excluded volume on the coil size of dilute linear polymers was investigated by off-lattice Monte Carlo simulations. The radius of gyration R_g was evaluated for a wide range of chain lengths at several temperatures and at the athermal condition. The θ temperature and the corresponding θ chain dimensions were established for the system, and the dependence of the size expansion factor, $\alpha_s = R_g/(R_g)_\theta$, on chain length N and temperature T was examined. For long chains and at high temperatures, α_s is a function of $N/N_s^\ddagger$ alone, where the length scale $N_s^\ddagger$ depends only on T. The form of this simulations-based master function compares favorably with $\alpha_s(M/M_s^\ddagger)$, an experimental master curve for linear polymers in good solvents, where $M_s^\ddagger$ depends only on polymer−solvent system. Comparisons when $N_s^\ddagger(T)$ and $M_s^\ddagger$(system) are reduced to common units, numbers of Kuhn steps, strongly indicate that coil expansion in even the best of good solvents is small relative to that expected for truly athermal solutions. An explanation for this behavior is proposed, based on what would appear to be an inherent difference in the equation-of-state properties for polymeric and monomeric liquids.

Introduction

Discussions about flexible-chain polymers in dilute solution are frequently phrased in terms of "good solvent behavior" and "θ condition behavior". It is easy enough to define the θ condition operationally. It is the state where the second virial coefficient for long linear chains of the species is zero and the root-mean-square radius of gyration R_g scales with molecular weight M in the random walk manner: $(R_g)_\theta \propto M^{1/2}$. Defining a good solvent is more difficult because there is no easily identifiable sign that indicates a special state or limiting condition. Conceptually, a "perfect" good solvent, commonly called an athermal solvent, is one for which the excluded-volume effects are derived entirely from the space-filling volume of the chain itself. In practice, good solvents encompass a range of states within which R_g for long chains is insensitive to temperature and scales with length over some experimentally accessible range in the self-avoiding walk manner: $R_g \propto M^\nu$, $0.58 < \nu < 0.60$. It has long been suspected, however, that data obtained in even the "best" good solvents are not in accord with the athermal idealization.[1−6] In 1988 Fujita[5] summarized the evidence, suggesting that excluded-volume effects in dilute solutions become observable only at chain lengths that are an order of magnitude or more beyond the expected range for truly athermal solvents.

In the preceding paper,[7] we reviewed the data relevant to volume exclusion for linear chains of several species in a variety of good solvents. The excluded-volume expansion factors for four properties—radius of gyration, second virial coefficient, intrinsic viscosity, and diffusion coefficient—were found to be expressible as universal functions of chain length, appropriately rescaled for each choice of polymer and solvent species. Thus, for chains beyond the oligomeric range,

$$\alpha_x = f_x(M/M_x^\ddagger) \tag{1}$$

in which x stands for one of the four properties, each function $f_x(\xi_x)$ is universal, and $M_x^\ddagger$ is the characteristic molecular weight for a polymer−solvent system that locates the onset of size expansion effect.

Experimental data described by eq 1 are consistent with the two-parameter theory of polymer solutions.[1] However, the observed forms of $f_x(\xi_x)$ do not agree with the commonly used two-parameter expressions, such as the Domb−Barrett (DB) equation.[8] Thus, the experimental crossover for the size expansion factor α_s—from unity for $M \ll M_s^\ddagger$ to $(M/M_s^\ddagger)^{\nu-1/2}$ for $M \gg M_s^\ddagger$—is more abrupt than that of the DB prediction. In addition, and especially relevant to the discussion here, the magnitudes of $M_x^\ddagger$ suggest a much weaker excluded-volume effect than the expectation for athermal solvents, consistent with Fujita's concern.[5] However, defining the athermal expectation is itself not a simple undertaking,[7] and as a result the general question of excluded-volume weakness remains unsettled.

In this paper we describe an off-lattice Monte Carlo simulation of self-excluding chains, undertaken in the hope of shedding additional light on the apparent weakness of excluded-volume interactions. The chains we consider are linear and self-avoiding, but they are also self-attracting and have an effective strength of attraction that varies with the temperature. Data on R_g vs N were gathered for various temperatures as well as for a purely repulsive (athermal) case. The excluded-volume effects were then organized in the manner used

† Current address: 7496 Old Channel Trail, Montague, MI 49437.

‡ Current address: Sandia National Laboratories.

10.1021/ma981915p CCC: $18.00
Published on Web 04/21/1999

previously for polymer solutions.[7] The θ condition was established, the results were used to determine $(R_g)_\theta$ vs N, and the size expansion factor, $\alpha_s = R_g/(R_g)_\theta$, was evaluated as a function of N at the other conditions. The correspondence between these results and the data for polymer solutions, including the possibility of master curve formation,

$$\alpha_s = f_s(N/N_s^{\ddagger}(T)) \tag{2}$$

were then considered in detail.

Simulation Model

Most numerical simulations of the polymer chain near the θ condition have been conducted on a lattice.[10−13] We used an off-lattice (continuum) model in which the polymer chain is represented as a string of $N + 1$ beads connected by rods of length σ. The beads are treated as soft spheres that interact in pairwise fashion through a modified Lennard-Jones potential:[14]

$$U(r) = 4\epsilon\left[\left(\frac{\sigma}{r}\right)^{12} - \left(\frac{\sigma}{r}\right)^{6} - \left(\frac{\sigma}{r_c}\right)^{12} + \left(\frac{\sigma}{r_c}\right)^{6}\right] \quad (r < r_c)$$

$$U(r) = 0 \quad (r > r_c) \tag{3}$$

Thus, the potential acts between all pairs of beads, ϵ characterizes the interaction strength, and r_c is the interaction cutoff distance.

When the interaction range r_c is truncated at $r_c = 2^{1/6}\sigma$, the potential is purely repulsive. The potential in this case is close to a hard-sphere condition, and we used it to approximate the athermal limit. In these simulations we use the temperature $T = \epsilon/k_B$, where k_B is the Boltzmann constant. Over a modest range, the choice of simulation temperature has little effect on the result because the repulsive potential is so steep. Thus, for example, the values of R_g for athermal chains with 400 and 800 beads are about 2% smaller at $T = 3\epsilon/k_B$ than at $T = \epsilon/k_B$.

To study behavior near the θ condition, it is necessary to extend the range of the interaction. In an earlier study of the collapse transition, Bäumgartner[15] set the cutoff to infinity. However, it is computationally more convenient to truncate the potential at some finite distance, as is done for all simulations on a lattice. In this study we set $r_c = 2.5\sigma$. Accordingly, it is possible to vary the relative importance of monomer−monomer attraction, and thus the solvent quality, by varying the temperature. Previous work on short chains[14] led to a value for temperature at the θ condition, $T_\theta = (3.0 \pm 0.1)\epsilon/k_B$. As seen below, this earlier value is an underestimate of the actual T_θ for the system.

In principle, the athermal condition could be examined without modifying the model at all, simply by raising the temperature sufficiently. The repulsive potential is not infinitely steep, however, so the effective "hard core" volume of the chain units would decrease with increasing temperature, making the analysis of data over a wide temperature range quite complicated. Experimentally, large variations of solvent quality are brought about not by varying temperature but by changing the solvent. Thus, the rather drastic procedure of using temperature alone is not even particularly realistic. Modifying the model slightly—cutting off attraction and employing a moderate temperature—is a reasonable alternative.

Table 1. Sizes and Expansion Factors for the Athermal Chain Simulations

$N + 1$	R_g^2/σ^2	$\langle R^2\rangle/R_g^2$	no. of attempts × 10^{-6}
2[a]	0.25	4	
4	0.78	5.62	1.0
8	2.12	6.36	2.0
16	5.4	6.59	1.0
32	13.6	6.56	1.0
64	32.9	6.52	1.0
100	57.1	6.45	1.0
200	134.8	6.39	2.0
400	311.7	6.37	8.0
800	714.6	6.33	12.0
1600	1638.4	6.30	16.0
3200	3723.6	6.29	16.0
6400	8472.1	6.28	16.0
12000	17803.8	6.27	20.0
24000	40325.0	6.27	20.0

[a] Calculated values—two identical mass points separated by unit distance.

In a continuum, as on a lattice, a computationally efficient method to measure R_g and $\langle R^2\rangle$ by Monte Carlo methods is the pivot algorithm.[16−20] In this procedure, a monomeric unit is selected at random, and one of the two segments formed by that partitioning is pivoted rigidly in a random direction about the unit. The energy of the new conformation is then calculated and compared to that of the previous conformation, and the new conformation is accepted or rejected based on a Boltzmann weighting factor. Madras and Sokal[18] have shown that this algorithm is ergodic and that it satisfies detailed balance. It is an efficient way to determine the average properties of dilute chains because each accepted move usually leads to a large change in chain conformation.[21]

We studied a range of chain lengths, from $N + 1 = 2$ to 24 000 for the athermal case and from $N + 1 = 16$ to 3200 for the various temperatures. For the athermal chains ($r_c = 2^{1/6}\sigma$; $T = \epsilon/k_B$) the values of R_g^2 (in units of σ^2), the ratio $\langle R^2\rangle/R_g^2$, and the number of attempted moves are given in Table 1.[22] Values of R_g^2 for the attractive case ($r_c = 2.5\sigma$ at the various temperatures) are given in Table 2. Typical runs ranged from 10^6 attempted moves for small N to 80 × 10^6 for large N near T_θ. Values of R_g^2/σ^2 are shown as a function of N for various temperatures in Figure 1.

Analysis of Data

Unperturbed Chain Properties. The θ temperature T_θ was determined by applying the following scaling equation relating R_g, N, and T near the θ condition:[12]

$$R_g^2 = Nf(\tau N^{1/2}) \tag{4}$$

in which $\tau = (T - T_\theta)/T_\theta$. Accordingly, near T_θ the values of R_g^2/N for various N and T should reduce to a function of $(T - T_\theta)N^{1/2}$ alone. For data in the ranges $200 \le N + 1 \le 3200$ and $3.0 \le T \le 3.6$, the choice of $T_\theta = (3.18 \pm 0.02)\epsilon/k_B$ was found by trial-and-error to produce the best reduction to this scaling form. This value is larger than the one reported earlier for the system.[14] The quality of agreement with the scaling form (eq 4) at $T = 3.18\epsilon/k_B$ can be judged from Figure 2.

The values of R_g at T_θ are the unperturbed dimensions needed to calculate size expansion factors. The

Table 2. Average Square Radius of Gyration for Self-Avoiding Chains at Various Simulation Temperatures[a]

	$N+1$								
$T(\epsilon/k_B)$	16	32	64	100	200	400	800	1600	3200
3.00	4.2	9.3	19.6	31.0	61.7	120.0	228.5	409.6	
3.05				31.8	63.7	124.2	245.5	456.8	785.2
3.10			20.1	32.2	65.7	130.1	255.1	476.4	944.1
3.15	4.3	9.5	20.3	32.6	67.3	133.9	269.8	514.4	1016.9
3.18[b]	4.3	9.5	20.4	32.9	67.6	137.6	272.9	548.8	1040.3
3.20	4.3	9.6	20.6	33.0	69.4	140.8	280.5	565.8	1168.4
3.30				33.6	71.1	148.4	308.0	616.4	1328.1
3.40	4.3	9.8	21.2	34.8	73.2	154.6	326.8	686.0	1431.0
3.50				35.4	75.3	159.4	342.0	718.7	1562.3
3.60	4.4	9.9	21.7	35.7	77.0	164.6	356.7	768.5	1630.5
3.80	4.4	10.1	22.5	37.3	81.4	176.6	380.0	832.2	1847.8
4.00	4.4	10.2	22.8	38.3	84.3	182.6	405.3	888.7	1958.4
4.50	4.5	10.5	23.8	40.0	89.2	199.8	442.3	986.7	2204.0
5.00	4.6	10.7	24.6	41.5	93.0	209.1	470.0	1055.3	2360.8

[a] Values of R_g^2 are expressed in units of square bond length σ^2. [b] Values for $N+1=4$ and 8 are 0.74 and 1.84.

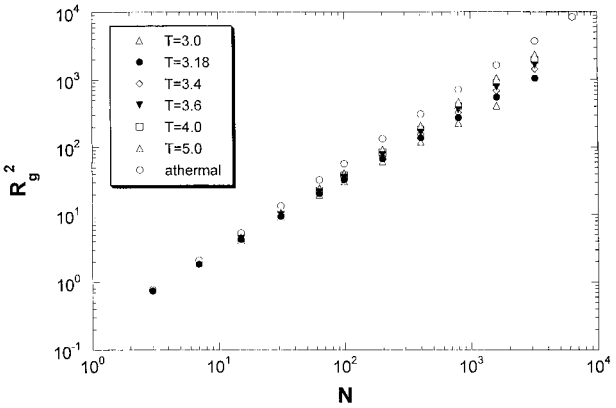

Figure 1. Mean-square radius of gyration as a function of chain length for various temperatures. Radius of gyration is expressed in bond length units in all the figures.

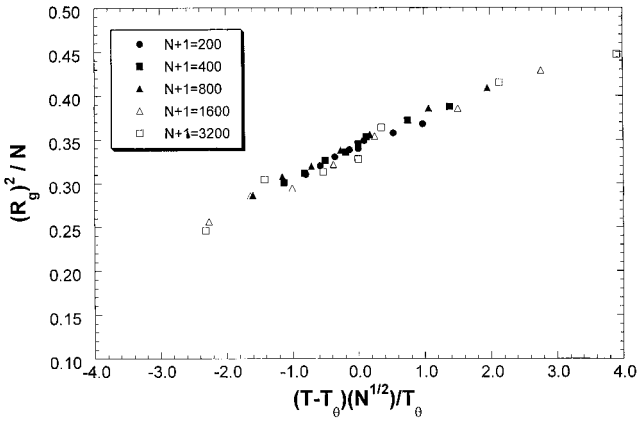

Figure 2. Test of the scaling relationship and establishment of the θ condition.

simulation was rerun at $T_\theta = 3.18\epsilon/k_B$ in order to obtain those values as accurately as possible. The results are listed in Table 2. The behavior of size in the T_θ vicinity is illustrated by the plots of R_g^2/N vs N in Figure 3. For long chains R_g^2/N is independent of N at T_θ, and the values for $200 \le N+1 \le 1600$ at T_θ are indeed consistent with that expectation. However, R_g^2/N at $N+1=3200$ is smaller by an amount (ca. 4.5%) that appears to be real, indicating perhaps that T_θ is slightly higher than $3.18\epsilon/k_B$. We chose simply to omit the size at $N+1=3200$ in the evaluation of unperturbed properties of long chains. Thus, R_g^2/σ^2 at $T_\theta = 3.18\epsilon/k_B$ is plotted as a function of chain length in Figure 4 with a best straight line of unit slope through the values for

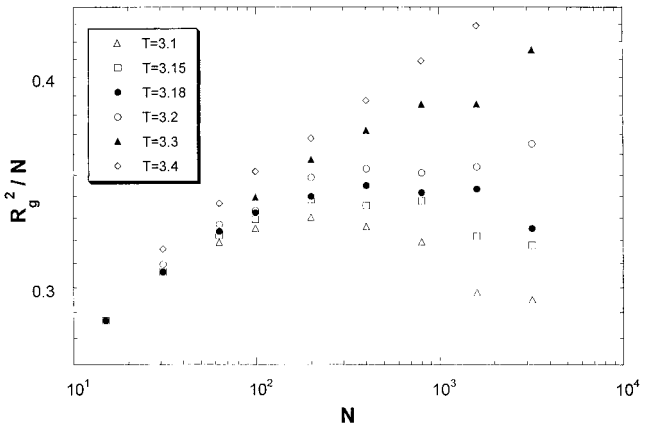

Figure 3. Values of R_g^2/N as a function of chain length in the θ region.

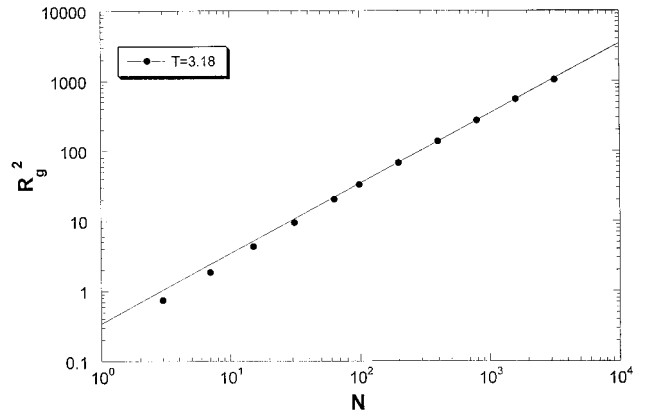

Figure 4. Mean-square radius of gyration as a function of chain length at $T_\theta = 3.18\epsilon/k_B$. The line is drawn with unit slope.

$200 \le N+1 \le 1600$, corresponding to

$$\left(\frac{R_g^2}{N}\right)_\theta = 0.343\sigma^2 \qquad (5)$$

This result is consistent with the value estimated as R_g^2/N at $N^{1/2}(T-T_\theta)/T_\theta = 0$ in Figure 2.

The backbone bonds of the chain have length $l_0 = \sigma$, so the value of $(R_g^2/N)_\theta$ for the corresponding set of random walks is $\sigma^2/6$. The characteristic ratio, $C_\infty \equiv (R_g^2)_\theta/(R_g^2)_{rw}$ in the long chain limit, is thus equal to $(0.343)(6) = 2.06$. Accordingly, the Kuhn length, $l_K \equiv C_\infty l_0$, is 2.06σ, and the number of Kuhn steps per chain,

$$N_K \equiv N/C_\infty \tag{6}$$

is equal to $0.486N$. Finally, we note that all values of $\langle R^2\rangle_\theta/(R_g^2)_\theta$ for $8 \le N+1 \le 1600$ are within about 1% of the random walk value of 6. The ratio is larger for the athermal chains, $\langle R^2\rangle/R_g^2 \sim 6.3$ in the range $800 \le N+1 \le 24\,000$ (Table 1), and the values are in excellent agreement with those for self-avoiding walks of similar lengths on a simple cubic lattice.[19]

Expansion Factor. For sufficiently long self-avoiding chains, R_g scales as N^ν. The exponent ν has been determined previously by careful Monte Carlo simulations. The most accurate values are 0.5877 by Li et al.[19] and 0.5876 by Nickel.[20] These results are in very good agreement with renormalization group estimates, which give $\nu = 0.5880$.[23] Though we did not try to simulate systems larger than $N+1 = 24\,000$, which is necessary for determining ν in the long-chain limit to such high precision,[24] our results for the athermal case are consistent with these results. Thus, Figure 1 shows that the power law is a reasonable approximation for the size−length relationship of the athermal case. The effective exponents decrease toward the expected value as chain length increases:

$$\nu_{\text{eff}} = 0.5964 \qquad 200 \le N+1 \le 6400$$
$$\nu_{\text{eff}} = 0.5914 \qquad 1600 \le N+1 \le 24\,000$$
$$\nu_{\text{eff}} = 0.5901 \qquad 6400 \le N+1 \le 24\,000$$

The trend is similar to that for the lattice walk data of Li et al.:[19]

$$\nu_{\text{eff}} = 0.5908 \qquad 400 \le N+1 \le 3500$$
$$\nu_{\text{eff}} = 0.5891 \qquad 1500 \le N+1 \le 25\,000$$
$$\nu_{\text{eff}} = 0.5885 \qquad 4500 \le N+1 \le 25\,000$$

The values of ν_{eff} over similar N ranges are smaller for the lattice walks, but the convergence rate is known to differ among self-avoiding systems.[24] The data in Table 1 in fact agree nicely with the crossover scaling form,[20,24] $R_g^2 = AN^{2\nu}(1 + BN^{-\Delta})$ for the choices $\nu = 0.588$ and $\Delta = 0.5$.

The size expansion factor, $\alpha_s = R_g(N,T)/R_g(N,T_\theta)$, was calculated for each N and T with the data in Tables 1 and 2. For $N+1 \le 1600$, $R_g(N,T_\theta)$ was taken to be R_g at $T = 3.18\epsilon/k_B$ in Table 2; for larger N it was calculated with eq 5. Results for the athermal case and at several temperatures are shown in Figure 5. Following the procedure described in the previous paper,[7] we examined the possibility of combining all data into a master curve by rescaling the lengths. We found that the data at higher temperatures can indeed be reduced in this way but that small systematic departures from superposability appear as the temperature is lowered.

The master curve formed by a rescaling of chain lengths for the high-temperature data, $3.8 \le T(\epsilon/k_B) \le 5.0$, is shown in Figure 6. Superposition is good, with the slight exception of the shortest chains at $T(\epsilon/k_B) = 3.8$, and shift factors relative to the $T = 5.0$ reference are well-defined. An attempt to form a master curve with the data at lower temperatures, $3.2 \le T(\epsilon/k_B) \le 3.6$, is shown in Figure 7. In this region, the values of α_s depart only slightly from unity for the largest available N, so well-defined shift factors would be difficult to assign even if superposition were valid. In fact, superposition breaks down, with the crossover becoming more gradual as the temperature is reduced.

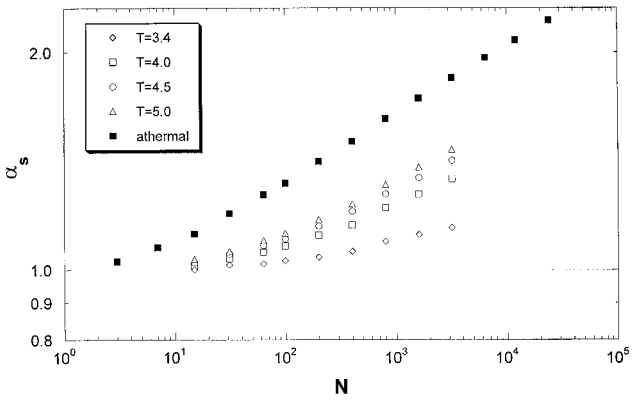

Figure 5. Size expansion factor as a function of chain length for various temperatures.

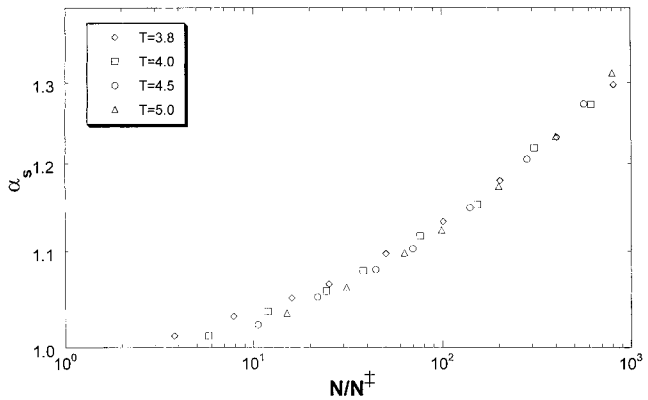

Figure 6. Master curve for the expansion factor at high temperatures.

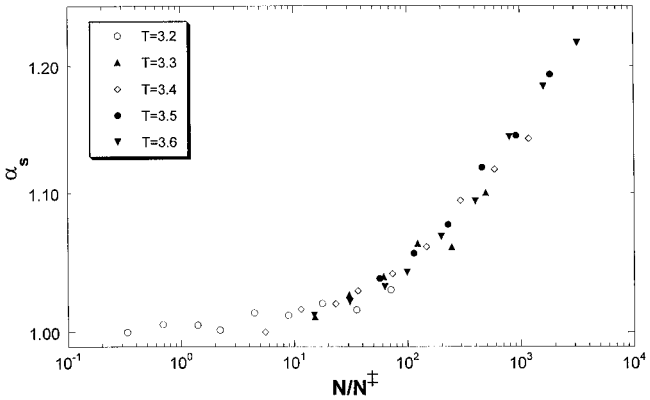

Figure 7. Attempted master curve for the expansion factor at low temperatures.

A composite of all results, now including the athermal data as well, is shown in Figure 8. It was obtained as follows. Shift factors for the lower temperatures were assigned visually, as a best-fit compromise with the $T = 3.6$ data and giving essentially the result shown in Figure 7. That result was then shifted to best superposition with the high-temperature master curve (Figure 6). The combined result was further shifted to best superposition with the athermal data. Only the athermal values for $N+1 \ge 16$ were used in this case. With the exception of a slightly low athermal value of α_s for $N = 15$, the agreement between the shifted high-temperature data and the athermal results is very good.

Finally, the overall shift factor for data at each temperature was used to establish $N_s^{\ddagger}$, the chain length

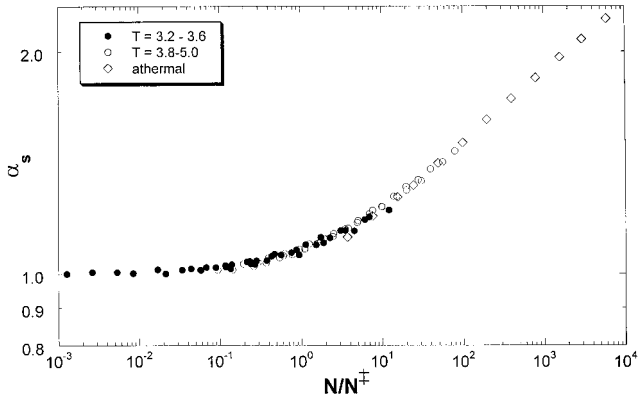

Figure 8. Expansion factor composite curve for all simulation data.

Table 3. Characteristic Lengths and Exclusion Parameters for Various Temperatures

$T(\epsilon/k_B)$	$N_s^{\ddagger}$	$N_K^{\ddagger}$ [a]	β/σ^3	β/β_{hs}
3.18	∞	∞	0	0
3.20	(11800)[b]	(5700)	(0.09)	(0.022)
3.30	(1700)	(830)	(0.17)	(0.042)
3.40	(700)	(340)	(0.27)	(0.064)
3.50	458	223	0.34	0.080
3.60	262	127	0.43	0.10
3.80	159	77	0.56	0.13
4.00	105	50.9	0.68	0.16
4.50	57.2	27.8	0.94	0.23
5.00	40.3	19.6	1.10	0.26
athermal	4.03	1.96	3.50	0.83

[a] Calculated with $N_K^{\ddagger} = 0.486N_s^{\ddagger}$, based on eq 6. [b] Values in parentheses are less certain than the others.

characterizing the onset of excluded-volume effects, in the manner used to establish $M_s^{\ddagger}$ in the previous paper.[7] Thus, a limiting power law, $\alpha_s = (\text{constant})N^p$, was estimated from the athermal data, taken as the reference, by a least-squares fit. Different exponents were obtained, depending on the range of N included in the fit. We settled on $p = \nu_{eff} - {}^1/_2 = 0.0915$, obtained by fitting the five largest sizes ($N + 1 \geq 1600$), and extrapolated back to the $\alpha_s = 1$ line to obtain $N_s^{\ddagger}$ for the athermal case. Values of $N_s^{\ddagger}$ at the various temperatures were then calculated from the athermal value by appropriate application of the various shift factors. The values of $N_s^{\ddagger}(T)$ so obtained are listed in Table 3.

The simulation results are compared in Figure 9 with the master curve for various polymer species in good solvents,[7] expressed in the units used here by the formula

$$\alpha_s^{5.46} - \alpha_s^{-20} = \left(\frac{N}{N_s^{\ddagger}}\right)^{1/2} \tag{7}$$

Also shown is the prediction of the Domb−Barrett interpolation formula, as modified in ref 7. Simulation and experiment agree rather well. Thus, the power law exponent from experiment, $p_s = 0.092$, is essentially the same as the one from simulation, $\nu_{eff} - {}^1/_2 = 0.0915$. The simulation would appear to cross over to the power law in a more gradual way than does eq 7, but the simulation departure is small compared with the uncertainty in the data upon which eq 7 is based. That aspect is seen more clearly in the direct confrontation of simulation data and experimental data[7] in Figure 10.

Excluded-Volume Parameter. In the previous paper,[7] values of β, the binary cluster integral for monomeric units, were obtained for various polymer−solvent systems with the approximation, $M_s^{\ddagger} = (M^{\ddagger})_{avg}$, and the following relationship, based on the Flory formula:[1]

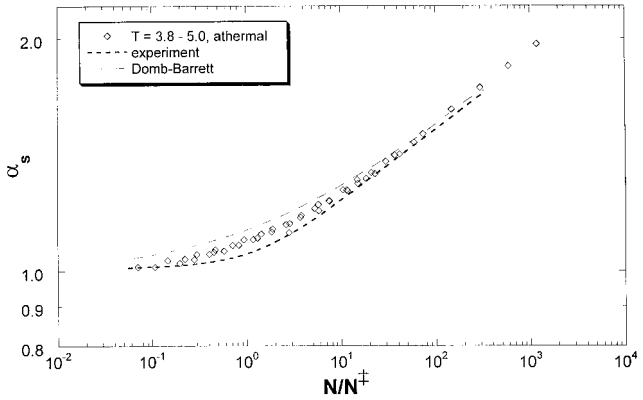

Figure 9. Comparison of high-temperature and athermal master curve data with the modified Domb−Barrett formula and an equation describing experimental data for polymer solutions.

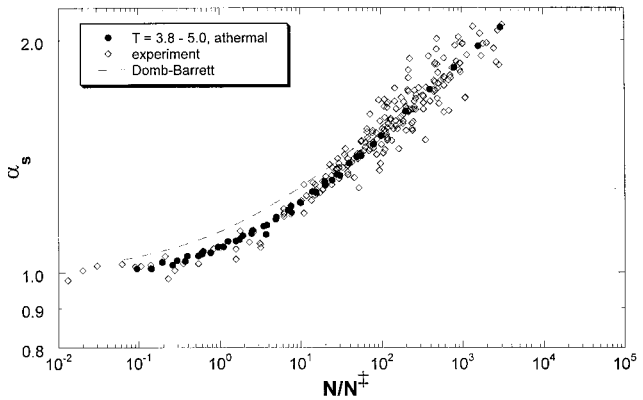

Figure 10. Direct comparison of master curve data from simulations and experiments.

$$\beta = \frac{(4\pi)^{3/2}}{1.276}\left(\frac{R_g^2}{M}\right)_{\theta}^{3/2} \frac{m_0^{\ 2}}{(M_s^{\ddagger})^{1/2}} \tag{8}$$

in which m_0 is the molecular weight per monomeric unit. The values so obtained were compared with β_{hs}, an estimated binary cluster integral for monomeric units modeled as hard spheres. Thus,

$$\beta_{hs} = 8v_0 \tag{9}$$

in which v_0 is the hard-sphere volume.

For applying the same analysis to the simulations, eq 8 becomes

$$\beta = \frac{(4\pi)^{3/2}}{1.276}\left(\frac{R_g^2}{N}\right)_{\theta}^{3/2} \frac{1}{(N_s^{\ddagger})^{1/2}} \tag{10}$$

for the binary cluster integral when expressed on a per-backbone-bond basis. As in the experimental study,[7] the effective hard-sphere representation to obtain β_{hs} is subject to some ambiguity. For the athermal case, the interaction is pure repulsion since the cutoff is $r_c = 2^{1/6}\sigma$. Thus, with a fixed bond length σ and making some allowance for the finite steepness of the repulsion, we assume that the equivalent hard core diameter is simply the bond length σ.

Table 4. Excluded-Volume Characteristics and Interaction Parameters for Various Polymer−Solvent Systems

polymer	solvent	$N_K^‡$	β/β_{hs}	χ^a	$\chi_{EXC}{}^b$	$\chi_{EOF}{}^c$
PS	benzene	14	0.13			
	toluene	17	0.12	0.44−0.48	0.004	0.37
	dichloroethane	22	0.11			
	ethylbenzene	31	0.089	0.40	0.02	0.53
	tetrahydrofuran	12	0.14			
PαMS	toluene	21	0.11			
a PMMA	acetone	61	0.056	0.48		
	nitroethane	12	0.13			
	chloroform	2.0	0.31	0.36_5		
	benzene	9	0.145	0.43		
i PMMA	acetone	160	0.052			
	nitroethane	19	0.15			
	chloroform	4.0	0.32			
PDMS	toluene	66	0.068			
	cyclohexane	31	0.10	0.42		
PIB	*n*-heptane	160	0.043	0.46	0.14^d	0.60^d
	cyclohexane	23	0.12	0.47	0.014	0.52
PI	cyclohexane	39	0.11	0.42	0.003	0.32
PBD	cyclohexane	108	0.14			
	tetrahydrofuran	67	0.18			

[a] Values from refs 20, 21, and 22. [b] Values calculated with the exchange interaction component of eq 13. [c] Values calculated with the equation-of-state component of eq 13. [d] Solvent was *n*-hexane instead of *n*-heptane.

Accordingly,

$$\beta_{hs} = \frac{4\pi\sigma^3}{3} \tag{11}$$

Values of β/σ^3 and β/β_{hs}, calculated with eqs 5, 10, and 11 for the various values of $N_s^‡$, are listed in Table 3. Values of $N_K^‡ = 0.486N_s^‡$ from eq 6 are also listed there.

The values of $M_{avg}^‡$ for the various polymer−solvent systems considered in the previous paper[7] were converted to values of $N_K^‡$ for purposes of comparing with the simulation results. The following relationship was used:

$$N_K^‡ = \frac{l_0^2}{6m_0^2}\left(\frac{M}{R_g^2}\right)_\theta M_{avg}^‡ \tag{12}$$

in which l_0 is the backbone bond length, m_0 is the molecular weight per backbone bond, the values of $(R_g^2/M)_\theta$ and $M_{avg}^‡$ were taken from Tables 2 and 4 in ref 7. (The values of $N_K^‡$ obtained with eq 12 were always within a few percent of those calculated with eq 6 from literature values of C_∞ for the various polymer species.) The values of β/β_{hs} from ref 7 are also shown in Table 4.

The values of β/β_{hs} for simulation and experiment are not precisely the same at the same value of $N_K^‡$, in part at least because of numerical uncertainty in the normalization factor β_{hs} for each. However, it is clear that both β/β_{hs} and $N_K^‡$ for the athermal simulation are of order unity. Among all the experimental systems, only PMMA−chloroform has values of β/β_{hs} and $N_K^‡$ approaching unity. The others are all nominally classified as good solvent systems, but judging by their values of β/β_{hs} and $N_K^‡$, they are quite far from the athermal range.

Discussion

There is obviously a strong resemblance between the simulation results at high temperatures and the experimental data for dilute solutions of polymers in good solvents.[7] In the variation of expansion factor with chain length, the various simulation temperatures correspond to the behavior for the various polymer−solvent systems. The relationships obtained in both cases obey the master-curve principle, and the simulation and experimental master curves are identical within the uncertainties, as shown by Figure 10. Thus, for the range of simulation conditions, flexible polymer species, and good solvent species considered here, coil expansion behavior beyond the oligomeric size range is universal. On the other hand, simulation data near the θ condition do not superpose with the high-temperature data, indicating, as others have noted,[9,19] that the two-parameter theory of polymer solutions is not generally valid.

The simulation data show that, with no compensating attraction between nonbonded chain units, the pair cluster integral β inferred from $N_s^‡$ is of the order of β_{hs}, the value calculated from the bare volume of a chain unit. Thus, $\beta/\beta_{hs} = 0.83$ for the athermal simulation. Among the polymer−solvent systems (Table 4), β/β_{hs} is about 0.3 for PMMA−chloroform, but the others have smaller values, ranging from 0.04 to 0.18 and corresponding to simulations that have significant attractive interactions, $3.3 < T < 4.0$ in Table 3. Comparison of experiment and simulation on the basis of $N_K^‡$, and with PMMA−chloroform omitted, lead only to a somewhat higher temperature range, $3.5 < T < 5.0$. All this would seem to indicate that athermal systems, those with purely hard-core repulsion between nonbonded chain units, are rare indeed among polymer−solvent systems. The excluded-volume effect in even the best of good solvents for the various polymer species is very far from the athermal limit.

This "intermediate" nature of typical good solvents can be expressed in another way, as the value of χ, the Flory interaction parameter for the polymer−solvent system. The values available for the systems considered here,[25−27] extrapolated to the low concentrations that typify polymer coil interiors, are listed in Table 4. The θ condition corresponds to $\chi = 0.5$ and the athermal limit to $\chi = 0$. The values for good solvent are all far from $\chi = 0$, ranging from $\chi = 0.365$ for PMMA−chloroform to $\chi = 0.48$ for PMMA−acetone.

All this raises the question, why are there essentially no examples at all of athermal polymer−solvent systems? Or, what amounts to the same question, why is the interaction parameter bounded so far away from zero? We suggest that this seeming anomaly is caused

by an inherent difference in the equation-of-state properties of monomeric and polymeric liquids. Various theories of thermodynamic interactions based on such differences have been developed.[28−30] All are based on a corresponding-states assumption, that the thermodynamic properties of dense liquids are universal functions of reduced pressure, temperature, and volume: $\tilde{P} = P/P^*$, $\tilde{T} = T/T^*$, and $\tilde{V} = V/V^*$. The species and composition dependence of properties is assumed to reside entirely in the reducing parameters: the characteristic pressure P^*, which mainly reflects the cohesive energy density of a liquid, and the characteristic temperature T^*, which depends strongly on its thermal expansion coefficient. The pure component reducing parameters, obtained by fitting *PVT* data, and some molecularly motivated mixing rule provide theoretical estimates of the solution properties.

The Flory−Orwoll−Vrij theory[29] leads to a relatively simple expression for χ in the dilute limit.[31] With some harmless simplifications, and to the leading terms in differences of P^* and T^* for the components,

$$\frac{\chi RT}{V_s} = [(P_s^*)^{1/2} - (P_p^*)^{1/2}]^2 + \frac{\alpha_s T P_s^*}{2(T_p^*)^2}[T_s^* - T_p^*]^2 \qquad (13)$$

in which s and p refer to solvent and polymer, and V_s and α_s are molar volume and thermal expansion coefficient. The first term on the right describes the exchange (EXC) interaction and is governed by the difference in $(P_s^*)^{1/2}$ and $(P_p^*)^{1/2}$, the solubility parameters of the components.[32] The second describes the equation-of-state (EOS) interaction. It is governed by the difference in T^* of the pure components and hence mainly by the difference in their thermal expansion coefficients. Given the wide choice of solvents available, matching the solubility parameters to make χ_{EXC} as near zero as desired, is relatively easy. However, the values of T^* appear to be systematically larger for polymeric liquids (see Tables VIII-1 and VIII-2 in ref 33), and it turns out to be virtually impossible to reduce the value of χ_{EOS} to zero. Values of χ_{EXC} and χ_{EOS} for several of the polymer−solvent systems in this study, calculated with the data in ref 33, are shown in Table 4. The values of χ_{EXC} are small in all cases; the values of χ_{EOS} dominate the observed magnitude of $\chi = \chi_{EXC} + \chi_{EOS}$.

The average thermal expansion coefficient for a wide range of nonpolar or weakly polar solvents for the polymers of interest here is $\bar{\alpha}_s = 1.2 \times 10^{-3}$ K^{-1} (see ref 34). For a range of nonpolar or weakly polar polymers above their glass transition temperatures, the average is significantly smaller, $\bar{\alpha}_p = 0.7 \times 10^{-3}$ K^{-1} (see ref 35). There is essentially no overlap of the two populations of expansion coefficients. The "generic" value, $\chi_{EOS} = 0.30$, obtained from these averages with eq 13, is consistent with the observed lower bound of the experimental values for χ.

Finally, we note that monomeric and polymeric liquids, under comparable conditions of intermolecular potentials and distances, might be expected to differ systematically in thermal expansion coefficient and hence in T^*. For polymeric liquids the distance between units in the chain direction is determined by covalent bond lengths, and these are essentially independent of temperature. The distances between their other neighbors, like all neighbors in monomeric liquids, are free to change with temperature by the usual thermal expansion. Thus, one might guess $\alpha_p/\alpha_s = {}^2/_3$, a value not very different from the observed value, $\bar{\alpha}_p/\bar{\alpha}_s = 0.58$. Such a possibility, that polymeric and monomeric liquids differ systematically in this way and that this difference affects their mixing properties, has probably occurred to others, but we have not found mention of it in the literature.

Acknowledgment. We are grateful to Guy Berry, Walther Burchard, Hiroshi Fujita, and Jacques Roovers for very helpful comments and discussions and to a reviewer for suggestions. We are also grateful to the National Science Foundation for financial support of this work through a grant to Princeton University (DMR93-10762) and for the REU supplement to that grant that provided summer support for R.C.H. Sandia is a multiprogram laboratory operated by Sandia Corporation, a Lockheed Martin Company, for the United States Department of Energy under Contract DE-AC04-94AL85000.

References and Notes

(1) Yamakawa, H. *Modern Theory of Polymer Solutions*; Harper & Row: New York, 1971.
(2) (a) Flory, P. J. *Discuss. Faraday Soc.* **1970**, *49* (general discussion), 81. (b) Domb, C. *Discuss. Faraday Soc.* **1970**, *49* (general discussion), 82.
(3) Norisuye, T.; Fujita, H. *Polym. J.* **1982**, *14*, 143.
(4) Yamakawa, H.; Shimada, J. *J. Chem. Phys.* **1985**, *83*, 2607.
(5) Fujita, H. M*acromolecules* **1988**, *21*, 179.
(6) Fujita, H. *Polymer Solutions*; Elsevier: Amsterdam, 1990.
(7) Hayward, R. C.; Graessley, W. W. *Macromolecules* **1999**, *32*, 3502.
(8) Domb, C.; Barrett, A. J. *Polymer* **1976**, *17*, 179.
(9) Yamakawa, H. *Helical Wormlike Chains in Polymer Solutions*; Springer-Verlag: New York, 1997.
(10) Kremer, K.; Bäumgartner, A.; Binder, K. *J. Phys. A* **1982**, *15*, 2878.
(11) Kolinski, A.; Skolnick, J.; Yaris, R. *Macromolecules* **1987**, *20*, 438.
(12) Batoulis, J.; Kremer, K. *Europhys. Lett.* **1988**, *7*, 683.
(13) Zifferer, G. *Makromol. Chem., Theory Simul.* **1993**, *2*, 653; **1994**, *3*, 163.
(14) Grest, G. S.; Murat, M. *Macromolecules* **1993**, *26*, 3108.
(15) Bäumgartner, A. *J. Chem. Phys.* **1980**, *72*, 871.
(16) Lal, M. *Mol. Phys.* **1969**, *17*, 57.
(17) MacDonald, B.; Jan, N.; Hunter, D. L.; Steinitz, M. O. *J. Chem. Phys.* **1985**, *A18*, 2627.
(18) Madras, N.; Sokal, A. D. *J. Stat. Phys.* **1988**, *50*, 109.
(19) Li, B.; Madras, N.; Sokal, A. D. *J. Stat. Phys.* **1995**, *80*, 661.
(20) Nickel, B. C., private communication, 1998.
(21) Usually the bond around which to pivot the chain is chosen randomly, by a pseudorandom number generator. However, this often leads to successive attempted moves that are close together. Nickel[20] suggested an alternative method, leading to successive moves that are maximally far apart. In this case, instead of a random number p between 0 and 1 to determine the next point for the ith pivoting attempt, one uses $p = i\tau - [i\,\tau]$, where $[\cdots]$ represents the nearest integer, and $\tau = (5^{1/2} + 1)/2$ is the golden mean. We employed this procedure in the present simulations.
(22) All results, except the athermal data for $N + 1 = 12\,000$ and 24 000, were obtained from runs on a single processor of either a DEC 625 MHz or SGI R10000 computer. The largest two athermal systems were run using a parallel code on 6−10 DEC processors. For $N + 1 = 6400$, a million steps took about 10 h on the DEC processor. For an attractive chain with $N + 1 = 3200$, a million steps took 3.8 h on the SGI and 3.2 h on the DEC processor. Since near the θ point we ran at least 80 million steps, each data point in this region took about 9 days of CPU time.
(23) LeGuillou, J. L.; Zinn-Justin, J. *J. Phys. (Paris)* **1989**, *50*, 1365 and references there to earlier work.
(24) Sokal, A. D. In *Monte Carlo and Molecular Dynamics Simulations in Polymer Science*; Binder, K., Ed.; Oxford University Press: Oxford, 1995; pp 47−124.
(25) Flory, P. J. *Discuss. Faraday Soc.* **1970**, *49*, 7.

(26) Casassa, E. F. *J. Polym. Sci., Symp.* **1976**, *54*, 53.
(27) Orwoll, R. A.; Arnold, P. A. In *Physical Properties of Polymers Handbook*; Mark, J. E., Ed.; American Institute of Physics: Woodbury, NY, 1996; Chapter 14.
(28) Progogine, I. *The Molecular Theory of Solutions*; North-Holland: Amsterdam, 1957.
(29) Flory, P. J.; Orwoll, R. A.; Vrij, A. J. *Am. Chem. Soc.* **1964**, *86*, 3515.
(30) Sanchez, I. C.; Lacombe, R. H. *Macromolecules* **1978**, *11*, 1145.
(31) Flory, P. J. *J. Am. Chem. Soc.* **1965**, *87*, 1833.
(32) Hildebrand, J. H.; Scott, R. L. *The Solubility of Non-Electrolytes*; Dover Publ.: New York, 1964.
(33) Prausnitz, J. M.; Lichtenthaler, R. H.; Gomes de Azeredo, E. *Molecular Thermodynamics of Fluid-Phase Equilibria*, 2nd ed.; Prentice Hall: Englewood Cliffs, NJ, 1986.
(34) Allen, G.; Gee, G.; Wilson, G. J. *Polymer* **1960**, *1*, 456.
(35) Orwoll, R. A. In *Physical Properties of Polymers Handbook*; Mark, J. E., Ed.; American Institute of Physics: Woodbury, NY, 1996; Chapter 7.

MA981915P